Video Article

Determination of Molecular Structures of HIV Envelope Glycoproteins using Cryo-Electron Tomography and Automated Sub-tomogram Averaging

Joel R. Meyerson[1,2], Tommi A. White[1], Donald Bliss[3], Amy Moran[3], Alberto Bartesaghi[1], Mario J. Borgnia[1], M. Jason V. de la Cruz[1], David Schauder [1], Lisa M. Hartnell[1], Rachna Nandwani[1,4], Moez Dawood[5], Brianna Kim[6], Jun Hong Kim[7], John Sununu[8], Lisa Yang[9], Siddhant Bhatia[10], Carolyn Subramaniam[1], Darrell E. Hurt[11], Laurent Gaudreault[12], Sriram Subramaniam[1]

[1]Laboratory of Cell Biology, Center for Cancer Research, National Cancer Institute, National Institutes of Health
[2]The Medical Research Council Mitochondrial Biology Unit, University of Cambridge
[3]National Library of Medicine, National Institutes of Health
[4]Massachusetts Institute of Technology
[5]William Fremd High School
[6]University of Virginia
[7]Duke University
[8]Yale University
[9]University of Notre Dame
[10]Washington University in St. Louis
[11]Bioinformatics and Computational Biosciences Branch, National Institute of Allergy and Infectious Diseases, National Institutes of Health
[12]Thomas Jefferson High School for Science and Technology

Correspondence to: Sriram Subramaniam at ss1@nih.gov

Abstract

Since its discovery nearly 30 years ago, more than 60 million people have been infected with the human immunodeficiency virus (HIV) (www.usaid.gov). The virus infects and destroys CD4+ T-cells thereby crippling the immune system, and causing an acquired immunodeficiency syndrome (AIDS) [2]. Infection begins when the HIV Envelope glycoprotein "spike" makes contact with the CD4 receptor on the surface of the CD4+ T-cell. This interaction induces a conformational change in the spike, which promotes interaction with a second cell surface co-receptor [5,9]. The significance of these protein interactions in the HIV infection pathway makes them of profound importance in fundamental HIV research, and in the pursuit of an HIV vaccine.

The need to better understand the molecular-scale interactions of HIV cell contact and neutralization motivated the development of a technique to determine the structures of the HIV spike interacting with cell surface receptor proteins and molecules that block infection. Using cryo-electron tomography and 3D image processing, we recently demonstrated the ability to determine such structures on the surface of native virus, at ~20 Å resolution [9,14]. This approach is not limited to resolving HIV Envelope structures, and can be extended to other viral membrane proteins and proteins reconstituted on a liposome. In this protocol, we describe how to obtain structures of HIV envelope glycoproteins starting from purified HIV virions and proceeding stepwise through preparing vitrified samples, collecting, cryo-electron microscopy data, reconstituting and processing 3D data volumes, averaging and classifying 3D protein subvolumes, and interpreting results to produce a protein model. The computational aspects of our approach were adapted into modules that can be accessed and executed remotely using the Biowulf GNU/Linux parallel processing cluster at the NIH (http://biowulf.nih.gov). This remote access, combined with low-cost computer hardware and high-speed network access, has made possible the involvement of researchers and students working from school or home.

Video Link

The video component of this article can be found at http://www.jove.com/video/2770/

Protocol

The approach described here was developed using a specific set of instruments, tools and software. Because all labs will not be using this same experimental setup, effort was made to generalize the approach where possible, and provide alternatives where this was not possible.

1. Preparing vitrified virus samples

In the following section vitrified grids are prepared using the FEI Vitrobot Mark III, a blotting and plunge freezing robot. See Iancu, *et al.* for a detailed protocol on using this system [7]. As an alternative to a robotic plunger, a guillotine-style or gravity plunger is perfectly sufficient [6].

In Sections 1.2. and 1.3. a Gatan Solarus 950 glow discharge unit is used to clean sample grids and increase their hydrophilicity, though any glow discharge device designed for use with electron microscopy grids can be substituted.

Though the amount of sample volume applied to the grid before blotting and plunge freezing should be in the range of 2 µL, the virus and protein-A gold colloid volume in the sample mixture will vary depending on the source. As such, it is likely that a range of virus and gold dilutions or ratios will have to be tested and imaged in the microscope, and an ideal mixture determined empirically. Note that when image data is acquired in Section 3, between 10 and 20 gold fiducial markers should be present for proper tilt series alignment.

Caution: This section describes the use of gaseous ethane, hydrogen, and oxygen which are highly flammable. Proper caution should be taken when using these gases. Additionally, care should be taken to handle virus samples in accordance with biosafety recommendations. Finally, always wear protective eyewear and clothing when handling liquid nitrogen (N_2) and ethane.

1. Prepare FEI Vitrobot Mark III by turning on its N_2 gas supply, installing the humidifier cartridge and then filling the cartridge with filtered deionized water. Power on Vitrobot and set its climate chamber temperature to 22 °C, target humidity to 100%, blotting time to 6 sec, and blot offset to -2 mm.
2. Power on the Gatan Solarus 950 glow discharge unit and open H_2 and O_2 canisters that supply the unit. Pre-clean specimen chamber by running glow discharge for 1 min at 50 Watts.
3. Arrange the desired number of holey carbon grids on a glass coverslip, carbon side up, and place inside glow discharge specimen chamber through the top loading door. Clean grids by running glow discharge for 6-10 sec at 25 Watts. (Note that the carbon side of the Quantifoil brand grids used in this protocol are matte in appearance. This will not be true for all commercial grids so it is best to obtain this information from the manufacturer.)
4. Place grid box(es) inside coolant container bowl, and thermal diffuser spindle on the central cup that sits within the coolant bowl. Slowly pour liquid N_2 into the bowl until vigorous bubbling subsides, indicating equilibrium between bowl and liquid. Maintain liquid N_2 level throughout the remainder of the procedure, taking care to keep it out of the central cup.
5. Attach one end of a plastic hose to the ethane gas canister, and the other end to a glass pipette. Hold glass pipette tip to bottom of central cup, establish a slow, steady ethane flow, and ethane will begin condensing. Continue filling until the central cup is full. Remove spindle from central cup.
6. Prepare sample mixture by adding 2 µL protein-A gold colloid fiducial to 10 µL AT-2 inactivated HIV-1 virus suspension. Gently pipette mixture to bring fiducials into solution. Keep on ice.
7. Grasp the outer rim of a grid with the specialized Vitrobot tweezers. Apply 2 µL of sample mixture to carbon side of grid. Immediately instruct robot to load sample into humidified climate chamber, blot and plunge freeze in liquid ethane.
8. Transfer vitrified grid to grid box. Repeat step 1.7. to produce the desired number of grids. When finished, tighten screws on grid box lid(s) then quickly transfer box(es) to small liquid nitrogen transport dewar.

2. Loading samples into transmission electron microscope

Throughout this section, the liquid N_2 level in the loading chamber should be monitored vigilantly, and liquid replenished as needed, to ensure that grid boxes remain immersed. Before bringing a tool into contact with a grid, cool it by submerging it in liquid N_2 until it equilibrates with the liquid. After each use, tools should be defrosted using a hot air gun.

Throughout this section the FEI Tecnai G2 Polara transmission electron microscope (TEM) is used in conjunction with a Gatan Cryo Workstation. While the principle of loading samples under liquid N_2 conditions is applicable to all cryo-electron microscopy work, the steps of this section are specific to the equipment used in the experiment. The steps used for different equipment will vary by manufacturer.

CAUTION: Throughout this section, always wear protective eyewear and clothing when handling liquid N_2.

1. Ensure that TEM Compustage does not contain a specimen cartridge, and that the specimen selection rod and insertion rod are below 110 K.
2. Cool and prepare Cryo Workstation for loading grids into specimen storage block, which is part of the sample selection rod.
3. Transfer the cooled (< 110 K) selection rod from microscope to Cryo Workstation.
4. Slide selection rod forward to insert selection block into nitrogen bath on Cryo Workstation. Remove all specimen cartridges from storage block using specialized cartridge-handling forceps. Place grid box(es) in loading workstation and loosen lid(s) with a screwdriver.
5. Use tweezers to remove grid from grid box and place in cartridge. Use the specialized C-clip placement tool to deposit a C-clip on top of grid, securing grid in cartridge.
6. Repeat step 2.5. until desired number of grids are in cartridges. Transfer cartridges to specimen selection block.
7. Prepare Cryo Workstation for removal of specimen selection rod. Slide selection rod back to remove selection block from nitrogen bath. Remove selection rod from Cryo Workstation and attach to TEM.

3. Acquiring cryo-electron microscopy data

During this section, the FEI Batch Tomography software interface is used to set up a batch file that stores the coordinates of all grid positions of interest. When instructed by the user, the Batch Tomography software will revisit each of the positions and will coordinate tilt series acquisition via Digital Micrograph. If this software is not available, the Leginon software package is viable free, open source alternative [13]. Imaging was done at 200 keV, using a Gatan Imaging Filter (GIF) with a post-GIF 2K x 2K CCD camera (Gatan).

1. Position Compustage such that electron beam passes through vacuum. Switch to high magnification (34kX) Exposure Mode and perform direct alignments.
2. Align zero loss peak on energy filter. (This provides the energy filter with a reference for electrons with zero energy loss.)
3. Move the Compustage to a grid area featuring carbon. In low magnification (4.5kX) Search Mode, use the Wobbler function to tilt the stage back and forth between +/-15°. Meanwhile adjust the Z-axis stage position until minimal stage shift is observed. (This positions the stage approximately at eucentric height). Disable Wobbler when no stage shift is observed.
4. Use the automated Eucentric Height function to refine the eucentric height. (This routine uses cross correlation to obtain a more accurate eucentric height than in step 3.3). Eucentric height is stored automatically for later reference by Batch Tomography software.

5. Find an area of interest featuring approximately three to six virions, and no less than ten fiducial markers. Add this grid position to the batch tomography file.
6. Repeat steps 3.4. and 3.5. until desired number of positions are designated. Define batch parameters (±60° with 2° tilt increments, 1-2 e-/Å^2 /tilt view) and run the batch.

4. Reconstructing cryo-electron tomograms

1. Align tilt series using automatic fiducial-based alignment in RAPTOR [1].
2. Reconstruct tomograms using R-weighted back projection in IMOD [8]. The standard file format for the resulting data volumes is the MRC file, with file extension .mrc.

5. Segmenting virion subvolumes and identifying spikes

This section uses a customized extension of IMOD that allows the user to designate virion subvolumes within the tomogram. In Section 6, the user defined virion boundaries are used as a surface along which spikes are automatically selected.

1. Open IMOD and load a tomogram populated with virions.
2. Navigate along the Z-axis of the tomogram until the central slice through one of the virions is located. Verify that the virion centroid has been identified. After doing so, deposit a virion marker. This marker will be used by the automated virion segmentation utility in Section 6.
3. Continue centroid designation until all virion volumes are identified.
4. Close tomogram and save marker set defining virion centroids. Repeat until virions have been designated in all tomograms.
5. Using IMOD, down-sample virion subtomograms by a factor of four.
6. Denoise virions using edge-enhancing anisotropic diffusion as implemented in IMOD.
7. Subject virions to unsupervised membrane segmentation using an energy-based three-dimensional approach (detailed in Bartesaghi *et al.* 2005) [3].
8. Spikes are identified at locations on the segmented virion surfaces corresponding to the local maxima of cross correlation between the particular location and a synthetic symmetric spike-like volume. Those locations above a specified threshold are added to a list of coordinates for putative spike subvolumes.

6. Classifying and averaging the particles

1. Computationally extract the tomogram subvolumes (100 x 100 x 100 voxels) at each location that was identified in step 5.8. (this is done without denoising or binning). The resulting collection of subvolumes contain the spike proteins that will be classified and averaged in the following steps.
2. Determine the orientations of the long axis of the spike using the normal to the automatically segmented membrane at the location of each spike. This approach provides initial estimates for two of the three Euler angles.
3. Randomize the remaining in-place rotation to prevent any possible bias in subsequent alignments.
4. Apply Euler angles to subvolumes, then translationally align the subvolumes to their cylindrically averaged global average to ensure they all share the same center of mass.
5. Remove the 10% of subvolumes that correlate most poorly with the updated global average. This is done to remove densities at greatest risk of being erroneously identified spikes.
6. Align and classify spike volumes without using external references and with proper accounting of the missing wedge (detailed in Bartesaghi *et al.* 2008) [4]. Progressively refine subvolume alignments and classify spike volumes at each iteration.
7. Three-fold symmetry should be clearly observed in the early stages of classification, and at the fourth iteration, 3-fold symmetry is imposed. At each round, the most well-defined classes are averaged and used as the reference for the next round.
8. Typically ˜4000 spikes should be selected for each dataset. Final density maps are obtained after ˜5-12 refinement rounds and will include contributions from ˜50% of sub-volumes in each dataset.

7. Coordinate fitting

1. The density maps resulting from step 6.8 are opened in UCSF Chimera [12].
2. Produce a simulated 20 Å map of the X-ray coordinates using Chimera or EMAN [10].
3. Dock coordinates into random orientations. Using Chimera's built in steepest-ascent local optimization, fit coordinates by performing multiples of 100 steepest ascent steps until convergence is obtained.

8. Representative Results

Using 3D averaging and coordinate fitting, a variety of HIV and SIV Env spike structures have been resolved. Presented in Figure 3A is the structure of the Envelope spike from the HIV-1 strain, BaL (purple). The spike has three-fold symmetry with dimensions of ˜ 120 Å as measured from the membrane to the spike apex, and a maximal width of ˜ 150 Å which tapers down to ˜ 35 Å at the base of the spike. As seen in Figure 3B, by combining the density map for trimeric Env determined using cryo-electron tomography with the crystallographically determined structure for monomeric gp120 (red, derived from PDB ID, 2NY7), we were able to obtain a working molecular model for the trimeric envelope glycoprotein complex (PDB ID, 3DNN) [9].

Our approach also allows for the structural analysis of complexes formed between trimeric Env and a variety of gp120-specific protein fragments and antibodies. An example of this, in which Env is complexed with the broadly neutralizing b12 Fab is shown in Figure 4A (the entire complex is shown in purple). In this figure, the extra density corresponding to b12 is seen projecting outward from the spike, and parallel to the membrane. Structural interpretations of such complexes can be extended to the molecular level by fitting the density maps with atomic coordinates for portions of the spike, bound to the corresponding ligand. As seen in Figure 4B, when this density map is fitted with coordinates of the gp120 spike protein (red, derived from PDB ID, 2NY7) bound by b12 Fab (white), the relative orientations of the three gp120 cores can be discerned (PDB ID, 3DNL). These conformational relationships are instructive for understanding how such ligands interact with the spike and interfere with virus activity. Some other structures of unliganded and liganded Env that have been resolved by the method presented here include those of HIV-1

R3A, SIV CP-MAC, SIVmneE11S and SIVmac239, the ternary complex between HIV-1 Bal Env, sCD4 and the 17b Fab, and SIV CP-Mac Env complexed to the 7D3 antibody [9,14].
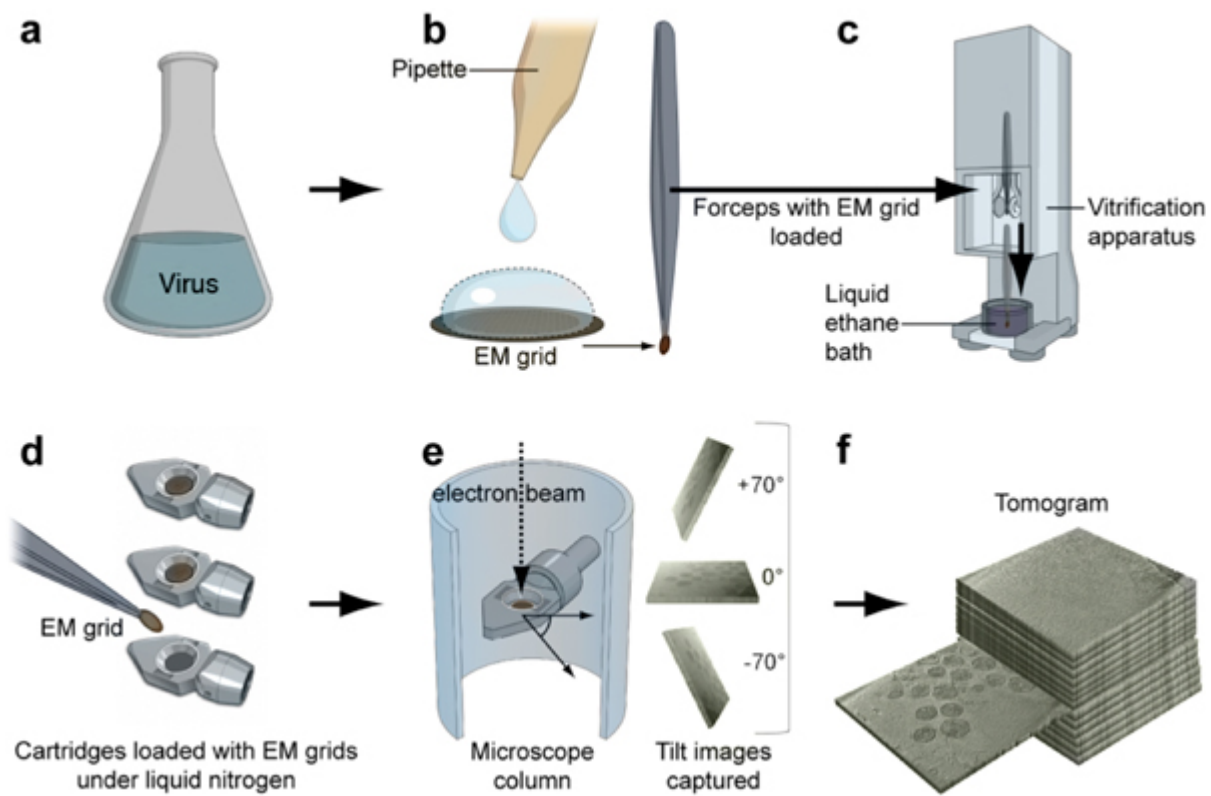

Figure 1. From viral suspension to 3D structure: conceptual steps in cryo-electron microscopy and 3D reconstruction.
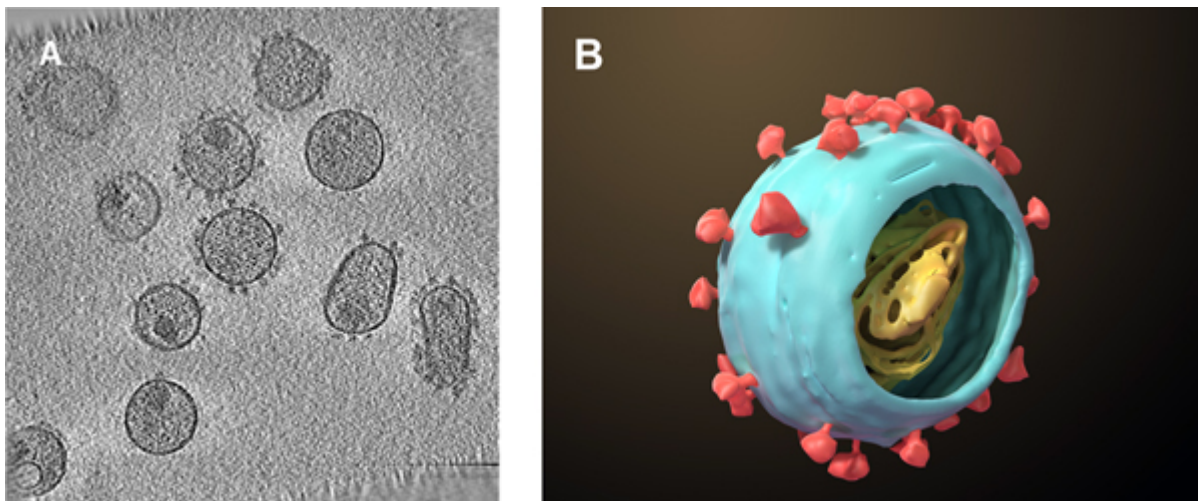

Figure 2. (A) A representative slice from a tomogram of HIV-1 virions. (B) A single HIV-1 virion, with the core and surface spikes shown schematically.
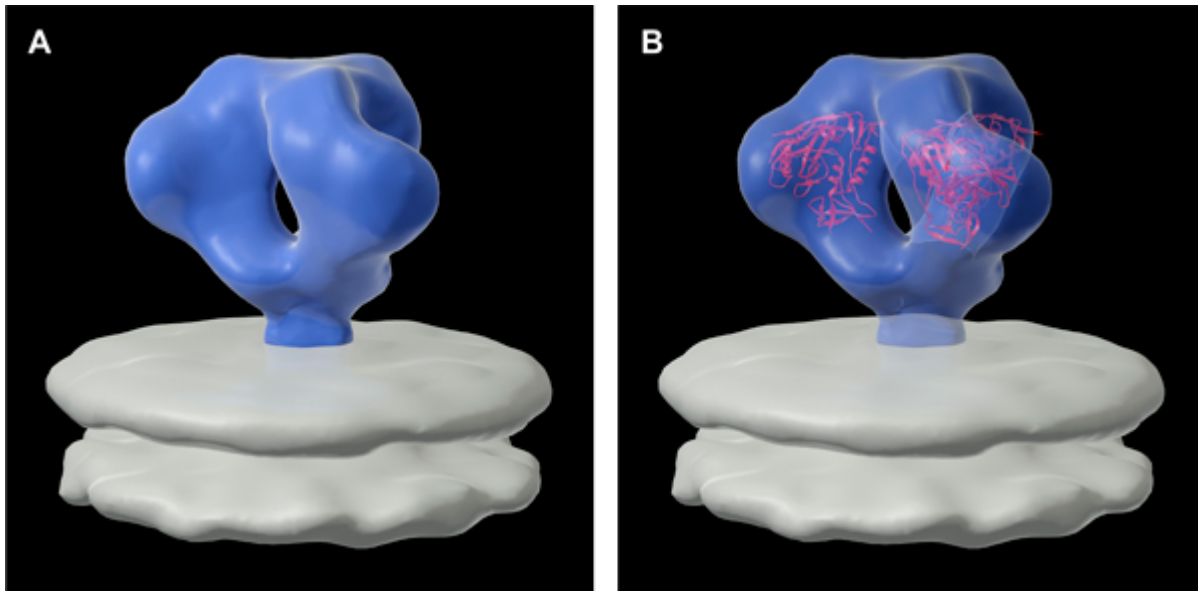
Figure 3. (A) Three-dimensional structure of the HIV-1 BaL Envelope glycoprotein (surface spikes) as displayed on the surface of the viral membrane. (B) Molecular model for the trimeric spikes determined by placing three copies of the structures for monomeric gp120 (red) derived by X-ray crystallography into the density map [9].
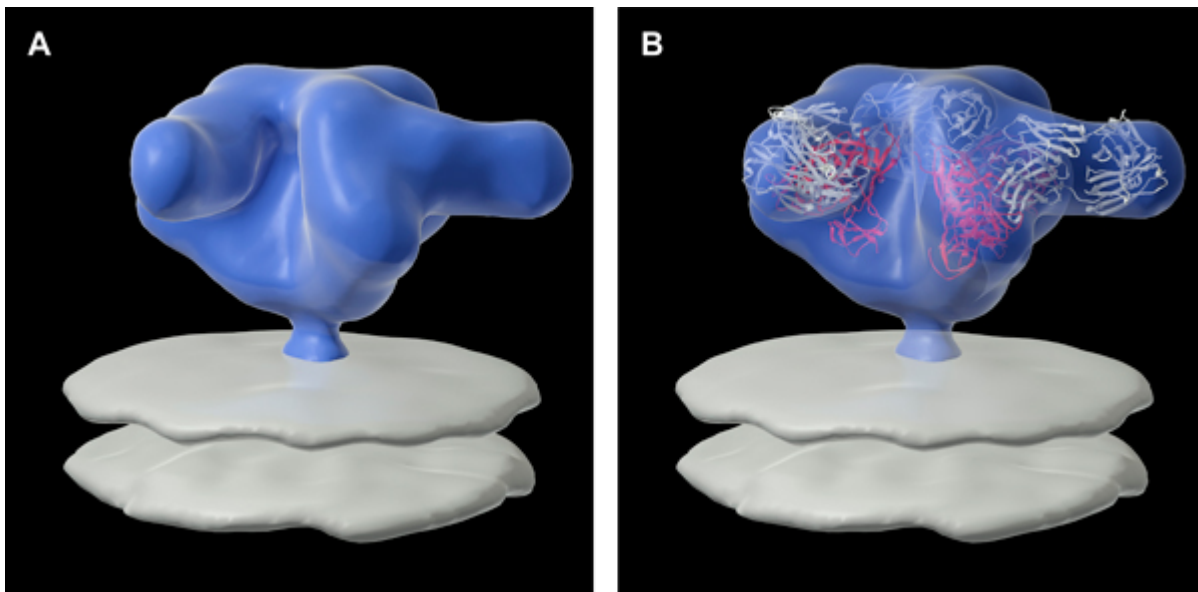

Figure 4. (A) Three-dimensional structure of HIV-1 BaL Envelope glycoprotein in complex with the Fab fragment of a broadly neutralizing antibody, b12. (B) Molecular model for the complex determined by placing three copies of the structures for monomeric gp120-B12 Fab complex derived by X-ray crystallography into the density map [9].

Discussion

The cryo-electron microscopy and three-dimensional classification and averaging methods presented here allow for the determination of three-dimensional structures of envelope glycoprotein complexes to ˜ 20 Å resolution. Fitting of X-ray coordinates of the monomeric components to the density maps allows for structural interpretation at the molecular level. Continuing improvements in low-cost computing equipment combined with developments in open source scientific tools and the proliferation of network infrastructure make possible previously unimaginable scientific collaborative endeavors. We take advantage of these developments and show that advanced scientific techniques can be brought within the reach of students of many ages.

Disclosures

No conflicts of interest declared.

Acknowledgements

References

1. Amat, F. *et al.* Markov random field based automatic image alignment for electron tomography. *J. Struct. Biol.* **161**, 260-275 (2008).
2. Bowen, D.L., Lane, H.C., & Fauci, A.S. Immunopathogenesis of the acquired immunodeficiency syndrome. *Ann. Intern. Med.* **103**, 704-709 (1985).
3. Bartesaghi, A., Sapiro, G., & Subramaniam, S. An Energy-Based Three-Dimensional Segmentation Approach for the Quantitative Interpretation of Electron Tomograms. *IEEE. T. Image. Process*. **14**, 1314-1323 (2005).
4. Bartesaghi, A., *et al.* Classification and 3D averaging with missing wedge correction in biological electron tomography. *J. Struct. Biol.* **162**, 437-450 (2008).
5. Harris, A., *et al.* Trimeric HIV-1 gp140 immunogens and native HIV-1 envelope glycoproteins display the same closed and open quaternary molecular architectures. *Proc. Natl. Acad. Sci. U.S.A.* **108**, 11440-11445 (2011).
6. Harris, R.J. & Adrian, M. Preparation of thin-film frozen-hydrated/vitrified biological specimens for cryoelectron microscopy. *Methods Mol. Biol.* **117**, 31-48 (1999).
7. Iancu, C., *et al.* Electron cryotomography sample preparation using the Vitrobot. *Nat. Protoc.* **1**, 2813-2819 (2006).
8. Kremer, J.R., Mastronarde, D.N., & McIntosh, J.R. Computer Visualization of Three-Dimensional Image Data using IMOD. *J. Struct. Biol.* **116**, 71-76 (1996).
9. Liu, J., Bartesaghi, A., Borgnia, M.J., Sapiro, G., & Subramaniam, S. Molecular architecture of native HIV-1 gp120 trimers. *Nature.* **455**, 109-113 (2008).
10. Ludtke, S.J., Baldwin, P.R. & Chiu, W. EMAN: Semiautomated Software for High-Resolution Single-Particle Reconstructions. *J. Struct. Biol.* **128**, 82-97 (1999).
11. Milne, J.L.S. & Subramaniam, S. Cryo-electron tomography of bacteria: progress, challenges and future prospects. *Nat. Rev. Microbiol.* **7**, 666-675 (2009).
12. Pettersen, E.F., *et al.* UCSF Chimera – A Visualization System for Exploratory Research and Analysis. *J. Comput. Chem.* **25**, 1605-1612 (2004).
13. Suloway, C., *et al.* Automated molecular microscopy: the new Leginon system. *J. Struct. Biol.* **151**, 41-60 (2005).
14. White, T., *et al.* Molecular architectures of trimeric SIV and HIV-1 envelope glycoproteins on intact viruses: strain-dependent variation in quaternary structure. *PLoS. Pathog.* **6**, e1001249 (2010).

December 2011 | 58 | e2770 | Page 6 of 6